COHERENT AND TURBULENT FLUCTUATIONS IN TFTR

K. McGUIRE, V. ARUNASALAM, M.G. BELL, M. BITTER, W.R. BLANCHARD, N.L. BRETZ, R. BUDNY, C.E. BUSH[1], J.D. CALLEN[2], M. CHANCE, S.A. COHEN, S.K. COMBS[1], S.L. DAVIS, D.L. DIMOCK, H.F. DYLLA, P.C. EFTHIMION, L.C. EMERSON[1], A.C. ENGLAND[1], H.P. EUBANK, R.J. FONCK, E. FREDRICKSON, H.P. FURTH, G. GAMMEL, R.J. GOLDSTON, B. GREK, L.R. GRISHAM, G. HAMMETT, R.J. HAWRYLUK, W.W. HEIDBRINK[3], H.W. HENDEL[4], K.W. HILL, E. HINNOV, S. HIROE[1], H. HSUAN, R.A. HULSE, K.P. JAEHNIG, D. JASSBY, F.C. JOBES, D.W. JOHNSON, L.C. JOHNSON, R. KAITA, R. KAMPERSCHROER, S.M. KAYE, S.J. KILPATRICK, R.J. KNIZE, H. KUGEL, P.H. LaMARCHE, B. LeBLANC, R. LITTLE, C.H. MA[1], J. MANICKAM, D.M. MANOS, D.K. MANSFIELD, R.T. McCANN, M.P. McCARTHY, D.C. McCUNE, D.H. McNEILL, D.M. MEADE, S.S. MEDLEY, D.R. MIKKELSEN, S.L. MILORA[1], D. MONTICELLO, A.W. MORRIS[5], D. MUELLER, E.B. NIESCHMIDT[6], J. O'ROURKE[7], D.K. OWENS, H. PARK, W. PARK, N. POMPHREY, B. PRICHARD, A.T. RAMSEY, M.H. REDI, A.L. ROQUEMORE, P.H. RUTHERFORD, N.R. SAUTHOFF, G. SCHILLING, J. SCHIVELL, G.L. SCHMIDT, S.D. SCOTT, S. SESNIC, J.C. SINNIS, F.J. STAUFFER[8], B.C. STRATTON, G.D. TAIT, G. TAYLOR, J.R. TIMBERLAKE, H.H. TOWNER, M. ULRICKSON, S. VON GOELER, F. WAGNER[9], R. WIELAND, J.B. WILGEN[1], M. WILLIAMS, K.L. WONG, S. YOSHIKAWA, K.M. YOUNG, M.C. ZARNSTORFF, S.J. ZWEBEN

Princeton Plasma Physics Laboratory,
Princeton University,
Princeton, New Jersey,
United States of America

[1] Oak Ridge National Laboratory, Oak Ridge, TN, USA.
[2] University of Wisconsin, Madison, WI, USA.
[3] GA Technologies Inc., San Diego, CA, USA.
[4] RCA David Sarnoff Research Center, Princeton, NJ, USA.
[5] Balliol College, University of Oxford, Oxford, UK.
[6] EG&G Idaho, Inc., Idaho Falls, ID, USA.
[7] JET Joint Undertaking, Abingdon, Oxfordshire, UK.
[8] University of Maryland, College Park, MD, USA.
[9] Max-Planck-Institut für Plasmaphysik, Garching, Fed. Rep. Germany.

Abstract

COHERENT AND TURBULENT FLUCTUATIONS IN TFTR.

Classification of the sawteeth observed in the TFTR tokamak has been carried out to highlight the differences between the many types observed. Three types of sawteeth are discussed: "simple", "small", and "compound". During the enhanced confinement discharges on TFTR, sawteeth related to q = 1 are usually not present, but a sawtooth-like event is sometimes observed. Beta approaches the Troyon limit only at low q_{cyl} with a clear reduction of achievable β_n at high q_{cyl}. This suggests that a β_p limit, rather than the Troyon–Gruber limit, applies at high q_{cyl} in the enhanced confinement discharges. These discharges also reach the stability boundary for $n \rightarrow \infty$ ideal MHD ballooning modes. Turbulence measurements in the scrape-off region with Langmuir and magnetic probes show strong edge density turbulence, $\tilde{n}/n = 0.3 - 0.5$, with weak magnetic turbulence, $\tilde{B}_\theta/B_\theta > 5 \times 10^{-6}$, measured at the wall, but these measurements are very sensitive to local edge conditions.

1. Introduction

Near-term achievement of ignition in tokamaks depends on overcoming anomalous heat conduction and/or control of the central energy transport due to sawteeth. Sawteeth in TFTR have been studied (Section 2) in an attempt to understand the mechanism that causes the sawtooth crash and gives rise to enhanced heat pulse propagation. The MHD activity observed in enhanced confinement discharges (locally known as supershots) and the constraints imposed by the Troyon and the β_p limit are discussed in Sections 3 and 4. In Section 5, a summary of turbulence measurements carried out on TFTR is presented, and the correlation between edge turbulence and gross confinement is examined. Finally in Section 6, we summarize the results of the coherent and turbulent fluctuations measured in TFTR.

2. Sawtooth Activity

Three types of sawtooth activity have been identified in TFTR: (1) simple or normal sawteeth, (2) small sawteeth, and (3) compound sawteeth. Simple sawtooth oscillations, as observed in most tokamaks, are a series of m/n = 0/0 relaxations, each with an m/n = 1/1 precursor mode, where m and n are poloidal and toroidal mode numbers, respectively. Figure 1a shows a simple sawtooth which is observed in TFTR plasmas with a small q = 1 radius and high q_a. Small sawteeth (Fig. 1b) are similar to simple sawteeth in period, but the m/n = 1/1 mode is different. While the precursor oscillations before the m/n = 0/0 crash are usually not present or have very small amplitude, the successor oscillations have a large amplitude. Compound (sometimes called "double") sawtooth activity (Fig. 1c) has been observed recently in many tokamaks [1-3]. Each compound sawtooth consists of a subordinate relaxation followed by a large (up to 20% in central T_e) main relaxation with a smaller inversion radius. Compound sawteeth appear frequently in ohmically heated plasmas with high plasma

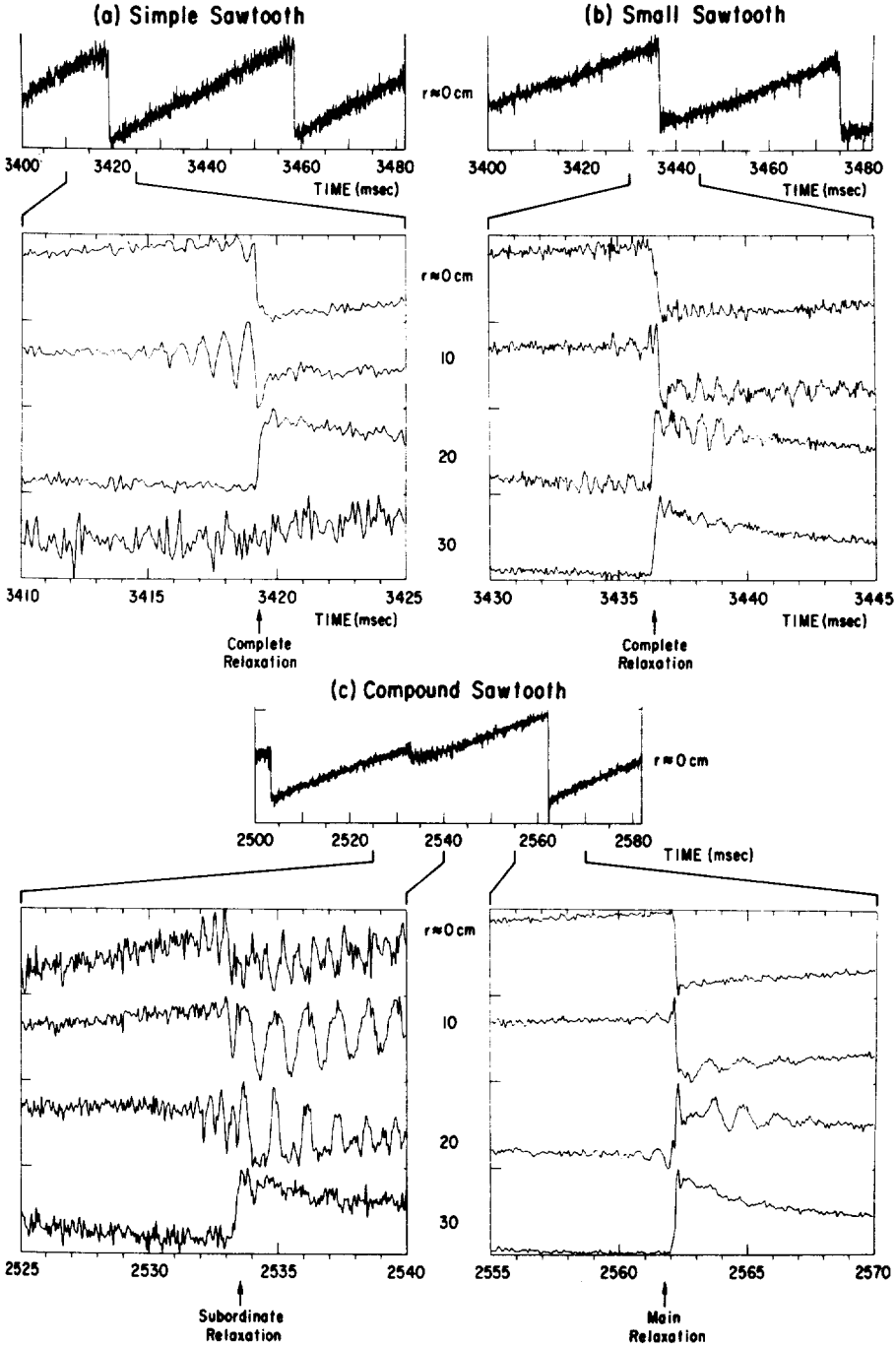

FIG. 1. Soft x-ray emissivity signals, indicating the three main types of sawteeth observed in TFTR. (a) Simple or normal sawtooth, (b) small sawtooth, and (c) compound sawtooth.

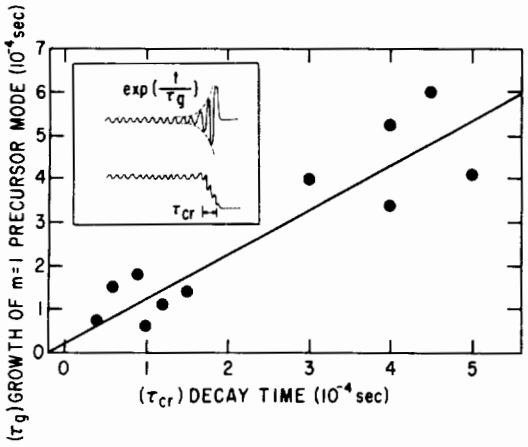

FIG. 2. Comparison between the growth time of the m = 1 mode at the crash of the sawtooth and the crash time of the sawtooth, as measured by the central soft x-ray signal.

current (I_p > 1.0 MA) and/or high density ($\bar{n}_e$ > 2.0 x 10^{19} m^{-3}). Sawteeth may switch from compound to small during the steady phase of a discharge, although global parameters such as averaged temperature, density, Z_{eff}, and even the inversion radius of the sawtooth do not change [2]. This suggests that small or localized changes of plasma parameters affect the characteristics of sawteeth significantly. The subordinate relaxation and the small amplitude of the m = 1 precursor indicate that compound sawteeth and small sawteeth cannot be explained by the Kadomtsev model [4]. It has been found that the duration of the crash (τ_{cr}) is proportional to the final growth time (τ_g) of an m = 1 mode during the crash phase itself (Fig. 2). Note that τ_{cr} appears to be completely determined by τ_g. Possible explanations include fast transport or reconnection due to: a) small perturbations at the q = 1 surface, b) two q = 1 surfaces [5] or c) a flat q profile with q_o close to 1 [1,6].

3. MHD Activity in Enhanced Confinement Discharges

Recent experiments on TFTR at low I_p and high-power balanced neutral beam injection (NBI) have achieved enhanced confinement relative to the predictions of L-mode scaling [7,8]. These discharges are remarkable from the MHD viewpoint, the most obvious feature being the lack of sawteeth during NBI for q_{cyl} > 5. This may be due to the removal of the q=1 surface from the plasma (some data show $r_{inv} \to 0$), but q_{cyl} < 5 enhanced confinement discharges with sawteeth have r_{inv} unchanged. During enhanced confinement plasmas with q_{cyl} > 5, there are occasional sawtooth-like events which are similar to the subordinate relaxations described in

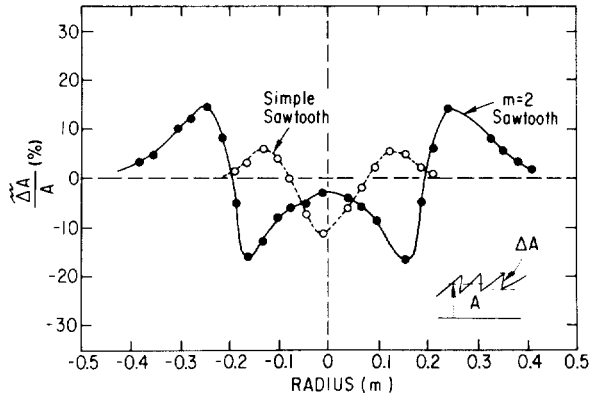

FIG. 3. Plot of ΔA/A of the sawtooth crash versus radius, for an m/n = 1/1 sawtooth in an L-mode, I_p = 900 kA discharge with 3.4 MW of counter NBI, and an m/n = 2/1 sawtooth in an I_p = 800 kA enhanced confinement discharge with 10 MW of balanced NBI. The m = 2 sawtooth-like event has an inversion at 0.2 m which is close to the calculated q = 2 radius.

Section 2. They have only a small perturbation on axis and an inversion close to the calculated location of the q = 3/2 or 2/1 surfaces. Figure 3 shows an m = 2 sawtooth-like event which was observed in an enhanced confinement discharge with I_p = 0.8MA, q_{cyl} = 7.6 and 10MW of balanced NBI; the calculated q = 2 radius for this discharge was about 0.25m. In Fig. 3 the line-averaged soft x-ray inversion radius was about 0.20m for the m = 2 sawtooth, which was larger than the m = 1 inversion radius observed at an m/n = 1/1 sawtooth in an I_p = 0.9MA, q_{cyl} = 7.3, and P_{inj} = 3.6MW counter-injection L-mode discharge. The mode amplitude and the phase on the x-ray diodes clearly show an m = 2 mode structure, also a small amplitude odd m-mode was present near the center. The magnetic signals at the wall show a clear m/n = 2/1 mode with no coupled mode structure. These m = 2 sawteeth are infrequent, with an irregular period, and they do not appear to affect the confinement of the discharge. The off-axis sawtooth events can occur during a period of continuous m/n = 3/2 or 2/1 activity (detected by magnetic measurements at the wall) with no interruption of the oscillation. Similar type sawteeth have also been observed in pellet injection discharges during a period of continuous m = 1 mode activity.

For identical operating conditions, enhanced confinement discharges can vary substantially, depending on the MHD activity. Figure 4 shows two such discharges, one with m/n = 2/1 activity, the other without MHD activity. The correlation of the MHD activity with the drop in total stored energy and neutron emission is very clear. This can occur with m/n = 2/1 alone, or m/n = 3/2 alone. Figure 5 shows the coherent MHD activity versus the rate

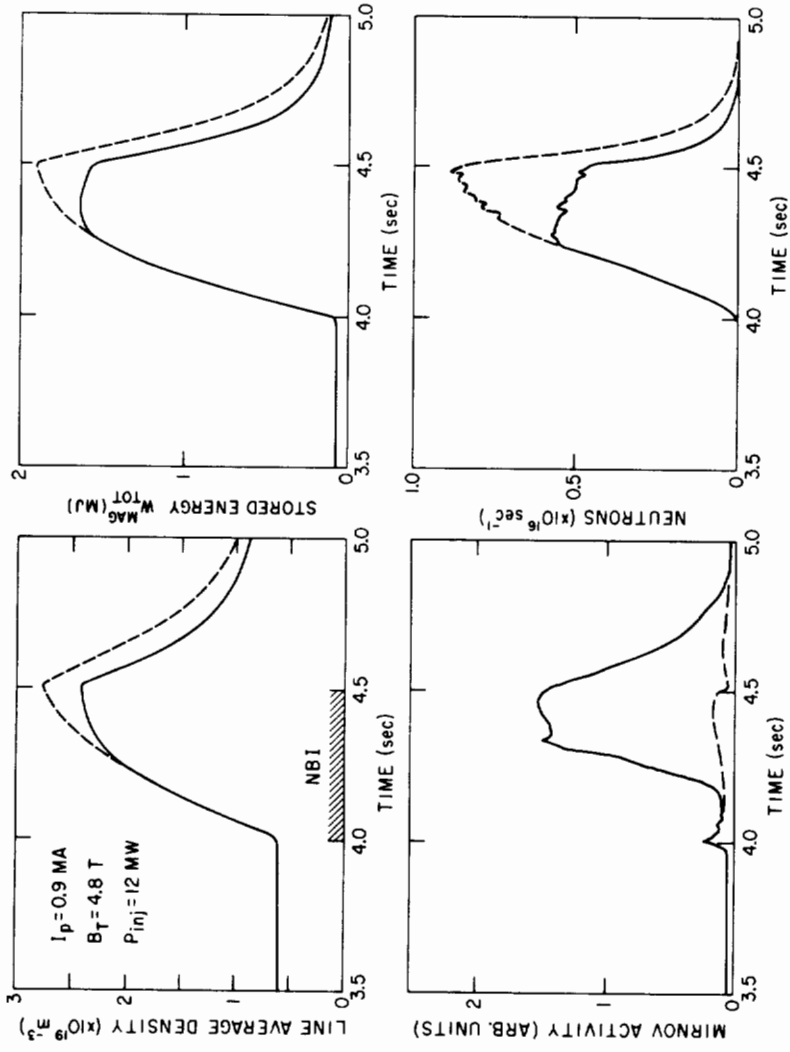

FIG. 4. Illustration of the effect of MHD activity on enhanced confinement discharges.

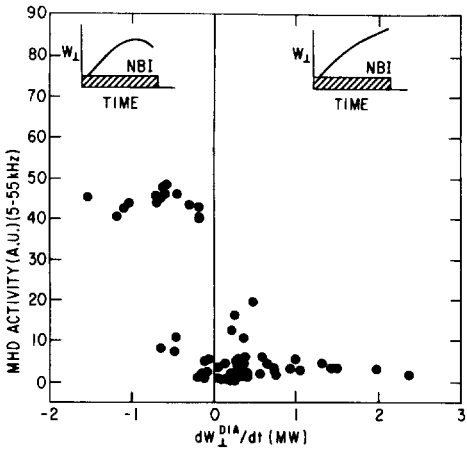

FIG. 5. MHD activity between 5 and 55 kHz versus $dW_\perp^{DIA}/dt$, 50 ms before the end of the beam pulse. These data include only enhanced confinement discharges. No similar correlation of MHD activity and confinement is seen for L-mode-type discharges.

of change of stored energy (calculated from the diamagnetic signal) 50ms before the end of the beam pulse. It is clear that a large amplitude of MHD activity is correlated with negative $dW_\perp^{DIA}/dt$. From delta-prime calculations on the j(r) profiles calculated by the TRANSP code [9] it is found that the profiles are sometimes unstable to the m/n = 2/1 and/or m/n = 3/2 modes. This implies that the j(r) profile may play an important role in the energy balance inside the q = 2 surface for the enhanced confinement discharges on TFTR [10].

At lower q_{cyl} ($< \sim 7$), bursts of m = 1 activity are seen in the center of the plasma on the soft x-ray detectors. This mode couples out as m/n ≈ 6/1 on the Mirnov coils, similar to the fishbone oscillations observed on PDX. This is in contrast with the 2/1 and 3/2 modes which appear as m/n = 2/1 and 3/2, respectively, on the Mirnov coils, even though the mode amplitude peaks at a similar radius (0.1 - 0.3 m). There is no measurable effect on the neutron emission, due to m = 1 activity at the levels observed to date, although we have observed coherent (5 kHz) oscillations in the charge-exchange neutral signals.

Enhanced confinement discharges which disrupt can lose most of the plasma energy in as little as 20 - 100 μs, with only a low amplitude or no detectable MHD activity preceding them. The temperature on the inner wall, as measured by 1.0 μm radiation, can rise to over 1200°C in 20 μs after a high β_p disruption. In a

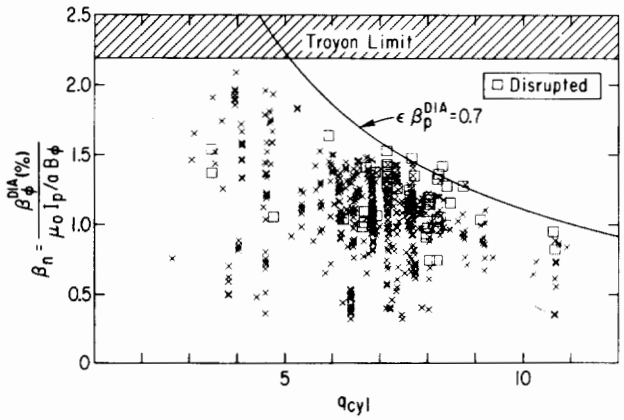

FIG. 6. The present enhanced confinement regime of TFTR on a plot of β_n versus q_{cyl}. The square symbols show discharges that disrupted during the neutral beam pulse. Also shown is a curve representing $\epsilon\beta_p^{DIA} = 0.7$, which fits the high q_{cyl} data better than the optimized Troyon limit.

few disruptive discharges, a 40 kHz mode growing on a 50 μs timescale, with an m = 1 structure in the center and m > 4, n = 1 on the magnetic signals, has been observed. Although the bulk of the plasma energy is lost rapidly, the current disruption occurs up to 0.5 s later, after a narrowing of the T_e and X-ray emission profiles. It is also observed that few major disruptions take place for $q_{cyl} < 5$; here the continuous 3/2 and/or 2/1 modes are detected and the energy is lost slowly, as in Fig. 4.

4. BETA Limits

Enhanced confinement discharges with $q_{cyl} < 5$ have values of normalized toroidal beta, $\beta_n = \beta_\phi/\beta_c$ ($\beta_c = \mu_0 I_p/aB_\phi$), which approach the limit found from optimized ideal MHD kink stability theory [11,12]. This limit has previously been confirmed on other devices with NBI (DIII, PDX, ASDEX, ISX-B, for example). The experimental limit from these devices is $\beta_n = 2.2 - 2.5$, approximately independent of plasma shape, but only for a small range of aspect ratio and q_{cyl}. Figure 6 shows β_n for the enhanced confinement regime of TFTR versus q_{cyl}. Diamagnetic β_ϕ^{DIA} (assuming a circular cross-sectional plasma) is used in Fig. 6 and, since the NBI is tangential, this underestimates the total β (< 10% at high β_p). It is seen that there is a clear fall of the achievable β_n with q_{cyl}. There is little published data from other auxiliary heated tokamaks in the high-β_n high-q region [13]. At high q_{cyl}, the limit appears to be disruptive, but at $q_{cyl} < 5$ the β_n limit is associated with coherent MHD activity. Attempts to reach higher β_n by reducing (I_p, B_ϕ) at constant q_{cyl} have not been successful. For a current ramp-down experiment with

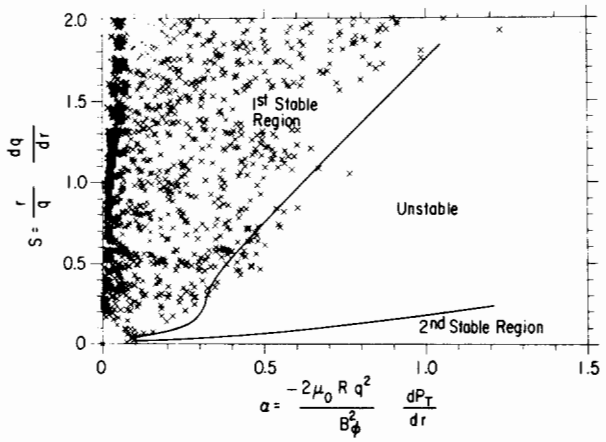

FIG. 7. Data from TFTR profiles on an S-α diagram for various types of discharge. The pressure profile used is the total pressure, $(P_\parallel + P_\perp)/2$, calculated by the TRANSP code [9].

NBI, β_p reached 2.65 before the discharge disrupted; this β_p was not maintained in equilibrium. There appears to be a hard β_p limit at 2 - 2.2 or an $\varepsilon\beta_p \approx 0.7$ limit, as illustrated in Fig. 6. However, the range of the inverse aspect ratio ε for the TFTR data is from 0.28 to 0.33 and it is not clear from this data whether ε is an important parameter in the β limit.

The profiles of enhanced confinement discharges have been examined for violation of the high-n ballooning mode stability criterion. Figure 7 shows points on the profile in the S-α diagram [14] (where $S = r(dq/dr)/q$, $\alpha = -2\mu_0 q^2 R(dP_T/dr)/B_\phi^2$) for various types of discharges. The pressure profile, $(P_\parallel + P_\perp)/2$ from the TRANSP code [9], which includes calculated beam and thermal ion pressure profiles and anisotropy, is used for dP_T/dr ($\alpha_{beam} \leq 0.7\,\alpha_{total}$). The beam-driven and bootstrap currents have been included in the calculation of q. The profile of maximum β_p hovers close to the curve for the large-aspect-ratio circular tokamak $n \to \infty$ ideal ballooning-mode stability limit [14]. Though the profiles may be at the ballooning limit, these discharges are not the optimum for $n \to \infty$ ballooning stability [15] (j(r) is not optimum). It is well known [16] that FLR, finite-n, toroidicity, and pressure anisotropy effects can all lead to significant movement of the stability boundary, and it is likely that TFTR is stable to modes with $n > 10$ under these conditions. Higher-n modes ($m > 3$ and $n > 3$) have been observed on soft x-ray diodes viewing the center of the plasma in TFTR at $q_{cyl} \approx 5 - 7$ and at high injection power. These high-n modes are not observed before disruptions at high β_p.

5. Turbulence in TFTR

Langmuir probes in the scrape-off region outside the last closed flux surface have revealed broadband turbulent fluctuations in the frequency range 10 - 200kHz, with fluctuation levels typically $\tilde{n}/n$ = 0.3 - 0.5 and $\tilde{\phi}/T_e$ = 0.1. Imaging of D-alpha light at the inner wall also shows large amplitude fluctuations [17] in this frequency range, with typical poloidal wavelengths λ_{pol} = 0.03 - 0.07m, but with λ_{tor} > 1.0m. Measurements of the magnetic fluctuations 0.11m outside the plasma edge show that the amplitude at 100kHz increases by a factor of 4 to $\tilde{B}_\theta/B_\theta = 5 \times 10^{-6}$ during neutral beam injection for both L-mode and enhanced confinement discharges. Since the distance of the coils from the plasma boundary varies for different coils, a radial e-folding distance can be measured; for most conditions this distance is about 0.05m. A strong dependence of the turbulent fluctuations on local edge conditions is found. For example, a gas puff of 5 Torr·l/s or a burst of low frequency m/n = 5/1 or 4/1 mode activity in an ohmically heated discharge can decrease the turbulent fluctuations by a factor of 10. From this result it is clear that turbulent fluctuations measured outside the plasma are not generally appropriate for direct correlation with global energy confinement.

The broadband spectra of $\tilde{n}$, $\tilde{\phi}$ and $\tilde{B}_\theta$ in the frequency range 10 - 250kHz have an approximate power-law dependence $P(f) \propto f^{\gamma}$, where $-1 > \gamma > -2$. Short radial decay lengths are found for $\tilde{n}$ and $\tilde{B}_\theta$ in the range corresponding to "mode numbers" m > 15, i.e., small-scale compared with the plasma size. The amplitude of the broadband fluctuations of $\tilde{n}$ and $\tilde{B}_\theta$ increased with NBI both in the L-mode and enhanced confinement mode.

6. Conclusions

On TFTR, three different types of sawteeth have been identified. The main differences are in the precursor and successor oscillation amplitudes. Possible explanations include extensions of the Kadomtsev model with two q = 1 surfaces and partial reconnection. Turbulence measured in the scrape-off region shows large amplitude fluctuations in the frequency range 10-250kHz, with fluctuation levels typically $\tilde{n}/n$ = 0.3-0.5 and $\tilde{\phi}/T_e$ = 0.1. It is also found that the measured edge fluctuations of $\tilde{n}$ and $\tilde{B}_\theta$ can be extremely sensitive to local edge conditions.

The enhanced confinement discharges on TFTR have values of β_n at low q_{cyl} which approach the limit found from ideal kink stability theory. At higher q_{cyl} it appears that the beta limit is better described by $\varepsilon\beta_p^{DIA} \approx 0.7$. In addition, dP_T/dr in these discharges is close to the $n \to \infty$ large aspect ratio ideal ballooning stability limit. High frequency modes at > 60kHz with m > 3, n > 3 have been observed in the core of discharges with

high β_p and high neutral beam power. Deterioration of confinement in the enhanced confinement discharges appears to be associated more with coherent modes (m/n = 2/1 and 3/2). Major disruptions at high β_p can have fast thermal energy decay (< 100 μsec); n = 1 modes (with many coupled m-modes) are sometimes observed, but high-n modes are not detected by the magnetic coils or soft x-ray diodes during these disruptions.

ACKNOWLEDGEMENTS

The authors are grateful to D.J. Grove and J.R. Thompson for their advice and support, and to J. Strachan for his many contributions.

This work was supported by the United States Department of Energy, under Contract No. DE-AC02-76-CHO3073. The ORNL participants were also supported by the United States Department of Energy, under Contract No. DE-AC05-840R21400 with Martin Marietta Energy Systems, Inc.

REFERENCES

[1] PFEIFFER, W., Nucl. Fusion **25** (1985) 673.
[2] McGUIRE, K., et al., in Controlled Fusion and Plasma Physics (Proc. 12th Europ. Conf. Budapest, 1985), Part 1, European Physical Society (1985) 134.
[3] CAMPBELL, D., et al., Nucl. Fusion **26** (1986) 1085.
[4] KADOMTSEV, B., Fiz. Plazmy **1** (1975) 710.
[5] DENTON, R., et al., Phys. Rev. Lett. **56** (1986) 2477.
[6] PARAIL, V., PEREVERZEV, G., Fiz. Plazmy **6** (1980) 27.
[7] HAWRYLUK, R.J., et al., Paper IAEA-CN-47/A-I-3, these Proceedings, Vol. 1.
[8] GOLDSTON, R.J., et al., Paper IAEA-CN-47/A-II-1, these proceedings, Vol. 1.
[9] HAWRYLUK, R.J., in Physics of Plasmas Close to Thermonuclear Conditions (Proc. Course Varenna, 1979), Rep. EUR/FU/BRU/XII/476/80, CEC, Brussels (1980) 503.
GOLDSTON, R.J., et al., J. Comput. Phys. **43** (1981) 61.
[10] FURTH, H., Plasma Phys. Controll. Fusion **28** (1986) 1305.
[11] TROYON, F., et al., Plasma Phys. Controll. Fusion **26** (1984) 209.
[12] MANICKAM, J., et al., Nucl. Fusion **24** (1984) 595.
[13] ROBINSON, D.C., et al., in Plasma Physics and Controlled Nuclear Fusion Research 1984 (Proc. 10th Int. Conf. London, 1984), Vol. 1, IAEA, Vienna (1985) 205.
[14] LORTZ, D., et al., Phys. Lett., A **68** (1978) 49.
CHOE, W., et al., Phys. Fluids **29** (1986) 1766.
[15] SYKES, A., et al., in Controlled Fusion and Plasma Heating (Proc. 11th Europ. Conf. Aachen, 1983), Pt. 11, European Physical Society (1984) 363.
[16] BISHOP, C., et al., Nucl. Fusion **24** (1984) 643.
TANG, W., et al., Nucl. Fusion **21** (1981) 891.
[17] ZWEBEN, S., et al., J. Nucl. Mater. **145–147** (1987).